Eur. Phys. J. A **25**, s01, 233–238 (2005)
DOI: 10.1140/epjad/i2005-06-118-9

EPJ A direct
electronic only

Fusion studies with RIBs

W. Loveland[a]

Oregon State University, Corvallis, OR 97331-4501, USA

Received: 12 September 2004 /
Published online: 29 June 2005 –

Abstract. Recent developments in fusion studies with radioactive beams are reviewed critically from the perspective of an experimentalist. Typical available radioactive beam intensities and purities are shown along with the methods used to study evaporation residues and fission fragments. The fusion of halo and other loosely bound nuclei, *i.e.*, ^{6}He, ^{11}Be, ^{17}F, is discussed. Fusion studies with intermediate mass beams such as ^{29}Al and ^{38}S are reviewed. Recent studies with n-rich fission fragments such as ^{132}Sn are shown. A discussion of fusion hindrance is presented and the use of radioactive beams in studying heavy nuclei is examined.

PACS. 28.52.-s Fusion reactors – 25.70.Jj Fusion and fusion-fission reactions

1 Introduction

Despite many years of study, fusion at energies near the Coulomb barrier is interesting to study because of the possibility of observing large enhancements in sub-barrier reactions that are related to nuclear structure and dynamics. These processes have been described as "coupling assisted tunneling". Studies with radioactive ion beams (RIBs) are especially interesting due to the unusual situations posed in fusion studies with halo nuclei (with their large radii that might enhance fusion and their weakly bound valence nucleons which may produce breakup). Also fusion studies with very n-rich RIBs may allow us to study neutron "flow" or transfer. I also include, in this review, fusion studies with radioactive targets (RTs). These RT studies represent a high luminosity extension of the RIB studies and in the heaviest nuclei, offer us the opportunity to study fusion phenomena under the influence of large Coulomb forces with a resulting complex dynamics. This review will be cursory and the reader is encouraged to look at more extensive reviews for details [1,2,3,4].

2 Experimental tools

In table 1, I show typical intensities of radioactive beams at Coulomb barrier (^{208}Pb) energies used in current studies of fusion. The beam intensities range from 10^3–10^6 particle/s. These low beam intensities preclude the usual "distribution of barriers" measurements [1] that typically require measurement of fusion cross sections to within 1% uncertainty in 1–2 MeV steps in excitation energy. Similarly the use of sweepers and other low efficiency experimental devices to detect evaporation residues is precluded. In all studies with RIBs, the issue of beam purity must be addressed. In my experience at a PF facility, MSU [5], or an ISOL facility, ORNL [6], beam contaminants of 10% of the total beam intensity can occur and must be tagged as part of a beam tagging system or tolerated because their reactions do not interfere with the primary measurement. In fig. 1, I show a typical plot of time of flight *vs.* energy for a near barrier ^{38}S beam at MSU showing a 10% contamination that was removed by tagging. A non-trivial aspect of RIB experiments is the so-called "misery coefficient", *i.e.*, the ratio of (number of hours spent waiting for beam due to accelerator problems)/(number of hours of useful beam on target). Regretably this quantity may significantly exceed unity.

Table 1. RIB intensities.

Projectile	Intensity (p/s)	Facility
^{6}He	10^5–5×10^6	Notre Dame
^{11}Be	4×10^4	RIKEN
^{11}Li	10^4	ISAC2
^{17}F	1.5×10^6	ORNL
^{38}S	5×10^3	MSU
^{46}Ar	4×10^3	MSU
^{132}Sn	5×10^4	ORNL

In detecting the products of fusion reactions, the most definitive quantity to be measured is the evaporation residue (EVR) production cross section as it is an unambiguous signature of fusion. For studies involving the

[a] e-mail: lovelanw@onid.orst.edu

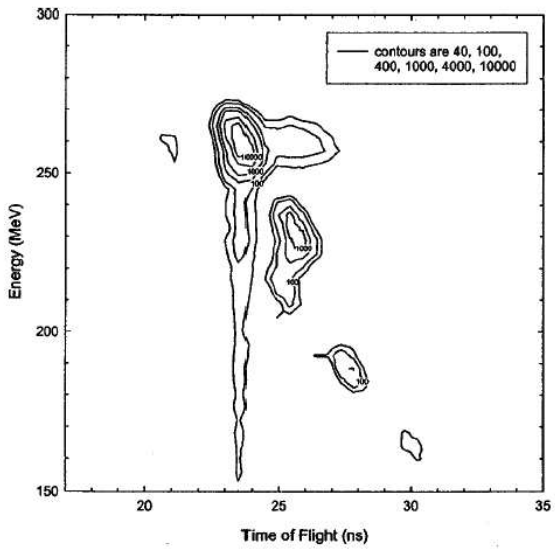

Fig. 1. Time of flight *vs.* energy for ^{38}S beam and impurities. The main peak at an energy of 260 MeV represents the ^{38}S beam, while the other peaks are those of contaminant beams. From Zyromski [5].

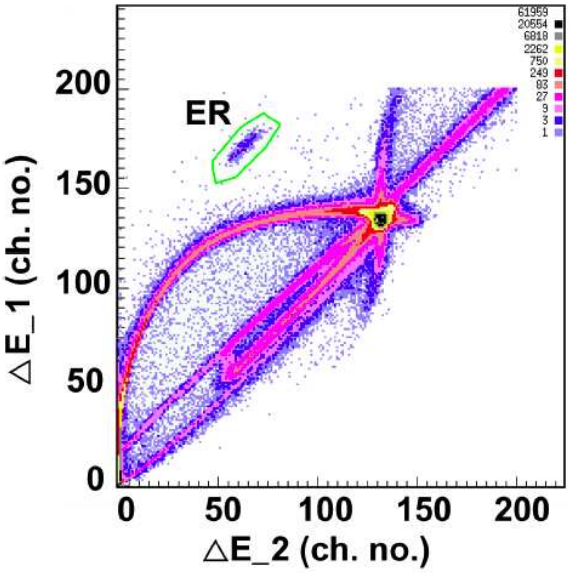

Fig. 2. Energy loss of beam and EVRs in two ion chamber segments. From Liang [6].

use of Pb or Bi targets, one can make the targets thick enough to stop the EVRs and detect their characteristic alpha-decay with the beam off. Shapira *et al.* [7] have constructed a high quality ion chamber that allows detection of evaporation residues emerging at zero degrees in a sea of scattered and direct beam particles (fig. 2). In some studies of fusion leading to heavier ERs, one chooses to detect fission fragments. They are relatively easy to detect with high efficiency and distinguish from scattered beam in asymmetric reactions in normal kinematics. Problems

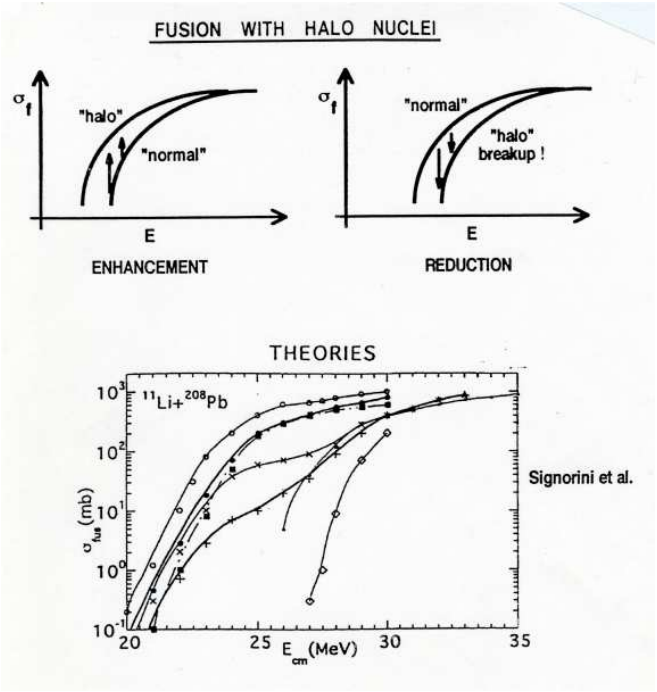

Fig. 3. Summary of theoretical predictions for the fusion excitation function for the ^{11}Li + ^{208}Pb reaction. From [9].

arise in inverse kinematics with n-rich fission fragment beams, especially if one wants to separate fusion-fission from quasifission and/or deep inelastic scattering [8].

3 Loosely bound nuclei

In studying the fusion of halo nuclei or other loosely bound nuclei, one is trying to assess the relative effects of any fusion enhancement due to the larger radii or any decrease in fusion due to projectile breakup. For the "Rosetta Stone" of such reactions, ^{11}Li + ^{208}Pb, there is a remarkable disagreement among theorists [9] as to what will happen, with estimates of the fusion cross section varying by several orders of magnitude at near barrier energies (fig. 3).

The ^{6}He + ^{209}Bi reaction has been extensively studied by Kolata and co-workers [10,11,12,13,14,15,16,17]. The fusion cross section for ^{6}He+^{209}Bi is substantially enhanced at sub-barrier energies compared to the ^{4}He+^{209}Bi reaction and reduced above the barrier (fig. 4). A similar result is seen for the ^{4,6}He + ^{238}U reaction [18,19] if one takes into account non complete fusion-fission reactions above the barrier. Alamanos *et al.* [20] were able to reproduce the excitation functions for these reactions using a coupled channels calculation where breakup of the ^{6}He projectile was simulated by reducing the real part of the entrance channel optical potential. Breakup processes were identified by direct detection of the incomplete fusion products by Dasgupta *et al.* [21] in the ^{6,7}Li + ^{209}Bi reaction resulting in a suppression of complete fusion by 66–74%.

For the reaction of the halo nucleus ^{11}Be with ^{209}Bi a complication arises in that the stable nucleus ^{9}Be used

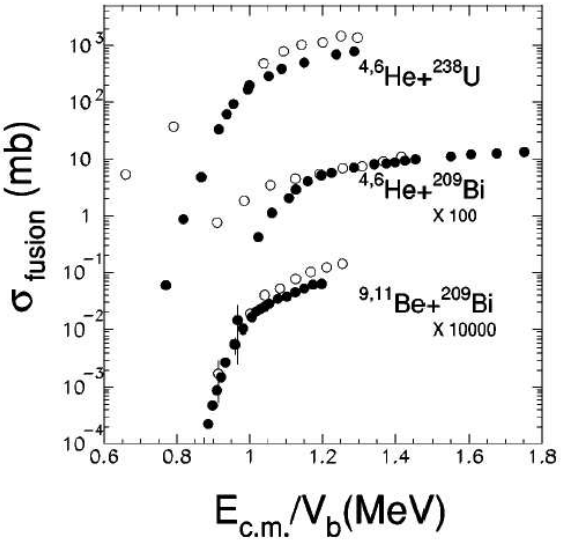

Fig. 4. Fusion excitation functions for loosely bound nuclei. The open circles indicate the RIB data while the closed circles indicate the stable beam data. From Alamanos [20].

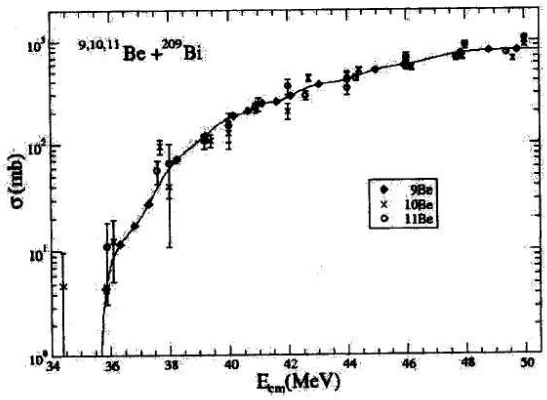

Fig. 5. Measured excitation functions for the ^{9,10,11}Be + ^{209}Bi reaction [22,23].

for comparison with the radioactive beam is very fragile itself, being one neutron outside of a ^{8}Be core and being deformed. The experimental data [22,23] show similar fusion excitation functions for the ^{9,10,11}Be + ^{209}Bi reaction, with no sub-barrier enhancement with ^{11}Be (fig. 5). (This is somewhat surprising given the halo structure of ^{11}Be and maybe due to a partial cancellation of enhancement and breakup effects.) Detailed calculations of the ^{11}Be fusion excitation functions considering breakup processes [20] do reproduce the observed cross sections.

The interaction of the single proton halo nucleus ^{17}F with ^{208}Pb was studied by Rehm *et al.* [24] who showed the excitation functions with ^{17}F and ^{19}F reactions to be identical when scaled by the differing reaction barriers. Breakup processes were deduced to be small, a conclusion verifed in a subsequent measurement by Liang *et al.* [25]. In summary of the data with light loosely bound nuclei,

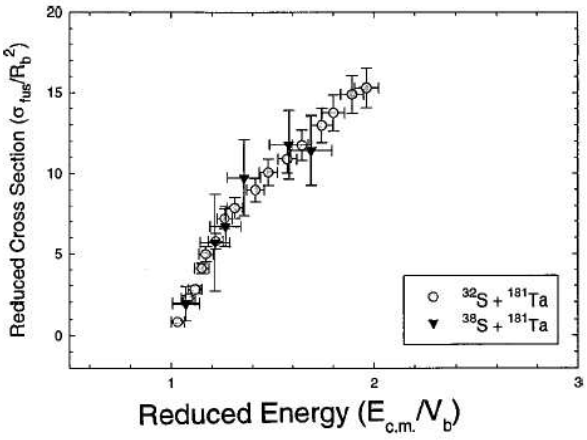

Fig. 6. Reduced excitation function for ^{32,38}S + ^{181}Ta. From Zyromski [5].

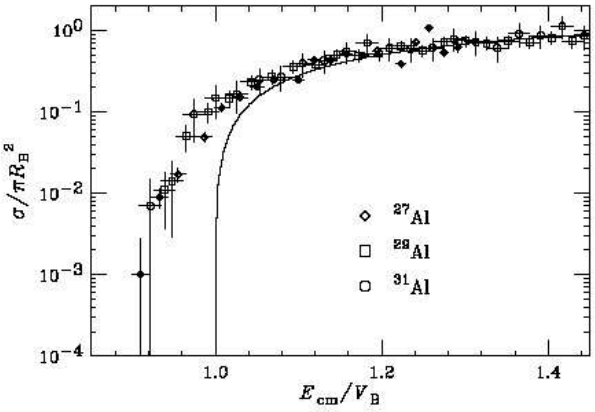

Fig. 7. Reduced excitation function for ^{27,28,29}Al + ^{197}Au. From Watanabe [26].

while there are experimental and theoretical points to be clarified, one concludes that, in the most well-studied system, there is fusion enhancement below the barrier due to couplings to transfer channels as well as bound states and suppression of fusion above the barrier due to breakup.

4 Intermediate mass neutron-rich nuclei

Zyromski *et al.* [5] found no fusion enhancement, other than the expected lowering of the fusion barrier for the n-rich ^{38}S, when comparing the fusion excitation functions of ^{32,38}S with ^{181}Ta (fig. 6). These measurements did not extend below the fusion barrier. In a similar study of the ^{27,28,29}Al + ^{197}Au reaction, Watanabe *et al.* [26] were able to make sub-barrier measurements. They also found that a reduced excitation function plot for the three systems studied showed no differences, apart from the expected barrier shift with the n-rich projectiles (fig. 7). Coupled channel calculations were not able to reproduce the sub-barrier cross sections, but the use of the Stelson model [27]

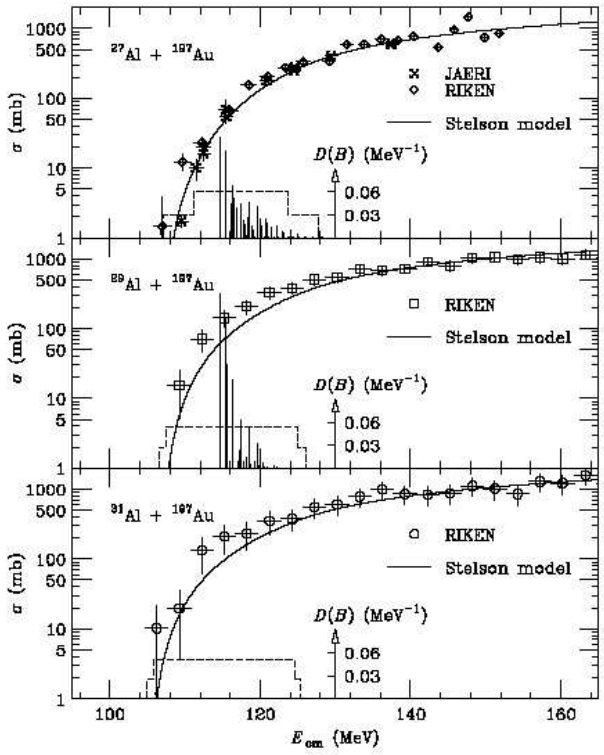

Fig. 8. Comparison of the measured fusion excitation functions with Stelson model calculations. The dashed lines show the barrier distributions, the vertical solid lines those calculated in CCDEF. From [26].

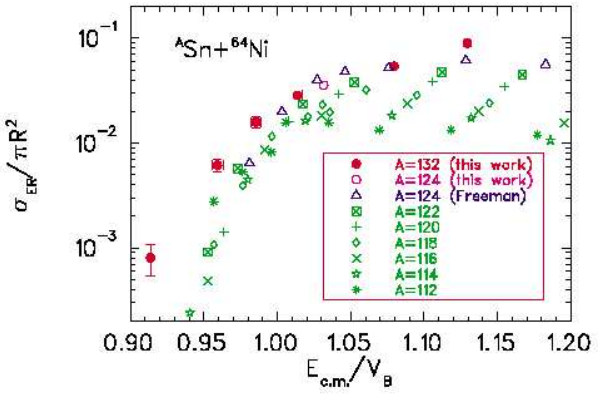

Fig. 9. Reduced excitation functions for $^{112-132}$Sn+^{64}Ni. From Liang [6].

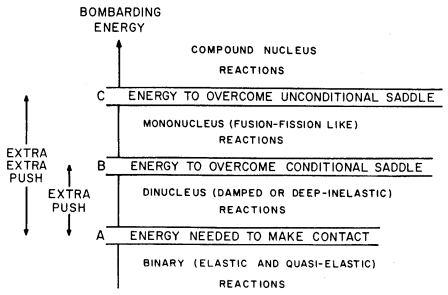

Fig. 10. Schematic illustration of the energies and reaction types involved in fusion hindrance. From Bjørnholm and Swiatecki [30].

to simulate neutron transfer processes was shown to reproduce the ^{27,28,29}Al + ^{197}Au and ^{38}S + ^{181}Ta data (fig. 8). (The Stelson model assumes a flat distribution of barriers and introduces the concept of an isospin dependent neutron flow in the collisions proceeding through neck formation in fusion.) In summary, the data on the fusion of intermediate mass, n-rich projectiles shows no evidence for unusual fusion enhancements apart from the expected barrier shifts, but does require neutron transfer or flow to explain the sub-barrier cross sections.

5 Heavy neutron-rich fission fragments

Liang *et al.* [6] studied the fusion of the n-rich fission fragment ^{132}Sn with ^{64}Ni in measurements of EVRs that went below the fusion barrier. When compared with previous measurements [28] of the fusion excitation functions for the $^{112-124}$Sn + ^{64}Ni reaction, a substantial sub-barrier fusion enhancement was observed that could not be explained by a simple shift of the fusion barriers with increasing isospin (fig. 9). Coupled channel calculations could not reproduce the ^{132}Sn excitation functions below the barrier although the inclusion of n-transfer channels did substantially improve the fit. A possibly relevant observation is that Wang *et al.* [29] were able to describe a similar situation in the ^{40,48}Ca + ^{90,96}Zr reaction using QMD calculations that included dynamical isospin effects on fusion. Extensions of these measurements to measure the fission exit channel in the ^{132}Sn + ^{64}Ni reaction and to study flow effects in the ^{134}Sn + ^{64}Ni reaction are underway [7,8].

6 Fusion hindrance $Z_1Z_2 \geq 1600$

When the charge product of the fusing nuclei Z_1Z_2 is greater than 1600, one observes fusion hindrance with the "missing" cross section going into quasifission ("fast fission"). This effect increases in importance with increasing values of Z_1Z_2 and is a very important limiting factor in fusion reactions to produce heavy nuclei. This effect was explained by Swiatecki and co-workers [30] in terms of the energetics of the collision (fig. 10). A certain amount of energy is needed to have the reacting nuclei come into contact (the "normal" reaction threshold) where neck growth between the nuclei starts. This results in elastic and quasielastic scattering and in some fusion models, fusion is defined as reactions proceeding beyond this point. An additional "extra push" energy is required to get the colliding nuclei to pass a conditional mass asymmetric saddle point, giving rise to deep inelastic events. Another energy, "the extra-extra push energy", is required to drive the system from the contact configuration inside the fission

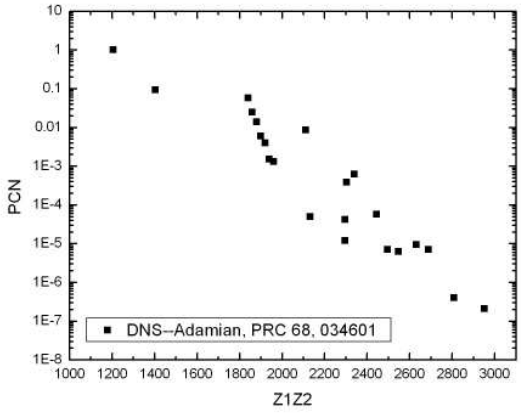

Fig. 11. DNS model calculations of $P_{\rm CN}$.

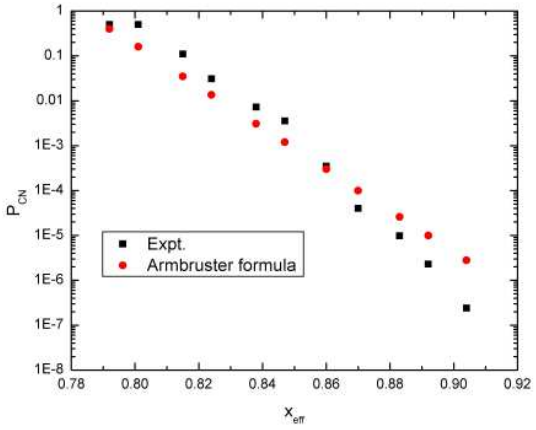

Fig. 12. Comparison of the Armbruster formalism with the measured EVR cross sections for the synthesis of elements 102–112.

saddle point where true complete fusion occurs. Systems that pass the conditional mass-asymmetric saddle but do not go inside the fission saddle point result in quasifission reactions. Reaction studies where $Z_1Z_2 \geq 1600$ in which one detects EVRs show an upward shift in fusion barrier (fusion hindrance) compared to unhindred systems.

There is no doubt about the occurrence of fusion hindrance in heavy systems but there are difficulties in characterizing it from both experimental and theoretical viewpoints. Two differing, mutually exclusive theoretical approaches have been used. In dynamical approaches [31] the reacting nuclei form a mononucleus which evolves past the fission saddle point (or fissions) that largely neglects the shell structure of the nascent fragments. An alternative approach [32] using the di-nuclear system (DNS) model proposes the reacting nuclei retain their identities well into the collision process with the reaction proceeding by nucleon transfer until the lighter nucleus transfers all of its nucleons to the heavier nucleus (compound nucleus formation) or re-separation before that happens. (Zagrebaev [33] has suggested a hybrid model.)

The underlying problem is the data used to check these predictions largely consists of EVR measurements in heavy nuclei where

$$\sigma_{\rm fusion} = \sigma_{\rm capture} P_{\rm CN} W_{\rm sur}\,, \qquad (1)$$

where $\sigma_{\rm capture}$ is the capture cross section (touching configuration), $P_{\rm CN}$ represents the probability that the nucleus will evolve from the contact configuration to inside the fission saddle point and $W_{\rm sur}$ is the survival probability (against fission) of any compound nuclei that are formed. It is difficult to unambiguously untangle $P_{\rm CN}$ and $W_{\rm sur}$. ($P_{\rm CN}$ is expected [32] to vary from 1 to 10^{-7} as Z_1Z_2 varies from 1200 to 2800 (fig. 11).) As a consequence, Zagrebaev *et al.* [34] have concluded that the fusion cross sections for reactions forming elements with $Z \geq 112$ can be estimated only within two orders of magnitude, at best. Nonetheless semiempirical treatments of $P_{\rm CN}$ exist with self-consistent evaluations of $W_{\rm sur}$ that allow one to describe heavy element formation cross sections for $Z \leq 112$ within an order of magnitude [35,36]. For example about 20 years ago, Armbruster [35] suggested a semi-empirical equation that defined $P_{\rm CN}$ as

$$P_{\rm CN}(E,J) = 0.5[\exp(c(x_{\rm eff} - x_{\rm thr}))], \qquad (2)$$

where the coefficient c has the value of 106 and the constant $x_{\rm thr}$ is 0.72 for actinide-based reactions and 0.81 for Pb or Bi targets. This equation describes the fusion reactions used to synthesize heavy nuclei (fig. 12).

The experimental signatures of quasifission involve an enhanced angular anisotropy [37] and large widths of the mass distributions. In systems where quasifission is the dominant process, complete fusion-fission events may be isolated as symmetric mass splits although that identification is not unambiguous. Measurements of the properties of quasifission, while interesting and informative in characterizing models of fusion, are unlikely to be executed with sufficient accuracy/precision to allow deduction of $P_{\rm CN}$ when that number $\ll 10^{-2}$.

7 RIBs and heavy nuclei

The use of neutron-rich RIBs to synthesize new heavy nuclei is a topic of interest to the nuclear science community. There are interesting opportunities for the use of neutron-rich RIBs, particularly in connection with the RIA project [38]. However there are some critical limiting factors. For production of new heavy nuclei in fusion reactions with ~ 1 pb cross sections requires beam intensities $\geq 10^{11}$ particles/s. That limits the radioactive projectile nuclei for a facility like RIA to be within 5–10 neutrons from stability. A more vexing, and as of yet, unresolved issue is that of the isospin dependence of fusion hindrance. Work done at GSI [39,40] indicates the more neutron-rich projectiles show a greater fusion hindrance (larger extra-extra push energies) than the more neutron-poor projectiles. For example, in fig. 13, one sees the extra-extra push energies in the ^{124}Sn+^{X}Zr reactions increase with increasing neutron number. Work is underway to study fusion hindrance in the ^{132}Sn + ^{90,96}Zr reaction [41].

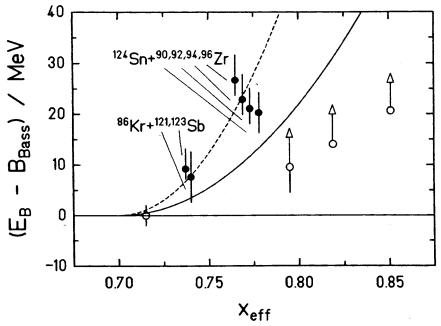

Fig. 13. Extra-extra push energies as a function of effective fissility. From Sahm [39].

8 Future developments

Some areas of possible progress in the next few years might include a) the full development and use of fission fragment RIBs to study fusion that will allow the use of normal kinematics and a wider variety of fused systems b) the development and use of ^{11}Li beams at the fusion barrier of nuclei like ^{208}Pb to resolve the questions posed by fig. 3 and c) more sophisticated measurements of fusion with high efficiency auxiliary detectors, such as neutron and gamma-ray arrays, allowing the detailed study of breakup processes and the identification of individual evaporation residues.

This work was supported in part by the U.S. Department of Energy, Office of High Energy and Nuclear Physics through Grant No. DE-FG06-97ER41026.

References

1. M. Dasgupta *et al.*, Annu. Rev. Nucl. Part. Sci. **48**, 401 (1998).
2. C. Signorini, Nucl. Phys. A **693**, 190 (2001).
3. R. Vandenbosch, `http://livingtextbook.oregonstate.edu/advanmat/nureactn/vandenbo.html`.
4. V.I. Zagrebaev, `http://nrv.jinr.dubna.ru/nrv`.
5. K.E. Zyromski *et al.*, Phys. Rev. C **63**, 024615 (2001).
6. J.F. Liang *et al.*, Phys. Rev. Lett. **91**, 152701 (2003).
7. D. Shapira, these proceeding.
8. J.F. Liang, these proceedings.
9. C. Signorini, Nucl. Phys. A **616**, 262c (1997).
10. J.J. Kolata *et al.*, Phys. Rev. C **57**, R6 (1998).
11. P.A. De Young *et al.*, Phys. Rev. C **58**, 3442 (1998).
12. J.J. Kolata *et al.*, Phys. Rev. Lett. **81**, 4580 (1998).
13. P.A. De Young *et al.*, Phys. Rev. C **62**, 047601 (2000).
14. E.F. Aguilera *et al.*, Phys. Rev. Lett. **84**, 5058 (2000).
15. J.J. Kolata, Phys. Rev. C **63**, 061604(R) (2001).
16. D. Lizcano *et al.*, Rev. Mex. Fis. **47**, 78 (2001); **46**, 116 (2000).
17. J.J. Kolata *et al.*, Eur. Phys. J. A **13**, 117 (2002).
18. M. Trotta *et al.*, Phys. Rev. Lett. **84**, 2342 (2000).
19. J.L. Sida *et al.*, Nucl. Phys. A **685**, 51c (2001).
20. N. Alamanos *et al.*, Phys. Rev. C **65**, 054606 (2002).
21. M. Dasgupta *et al.*, Phys. Rev. C **66**, 041602(R) (2002).
22. C. Signorini *et al.*, Eur. Phys. J. A **2**, 227 (1998).
23. C. Signorini *et al.*, Nucl. Phys. A **735**, 329 (2004).
24. E. Rehm *et al.*, Phys. Rev. Lett. **81**, 3431 (1998).
25. J.F. Liang *et al.*, Phys. Rev. Lett. **67**, 044603 (2003).
26. Y.X. Watanabe *et al.*, Eur. Phys. J. A **10**, 373 (2001).
27. P.H. Stelson *et al.*, Phys. Rev. C **41**, 1584 (1990).
28. W.S. Freeman *et al.*, Phys. Rev. Lett. **50**, 1563 (1983).
29. N. Wang *et al.*, Phys. Rev. C **67**, 024604 (2003).
30. S. Bjørnholm, W.J. Swiatecki, Nucl. Phys. A **391**, 471 (1982).
31. Y. Abe *et al.*, Nucl. Phys. A **722**, 241c (2003).
32. G.G. Adamian *et al.*, Phys. Rev. C **68**, 034601 (2003).
33. V. Zagrebaev, Phys. Rev. C **64**, 034606 (2001).
34. V.I. Zagrebaev *et al.*, Phys. Rev. C **65**, 014601 (2001).
35. P. Armbruster, Annu. Rev. Nucl. Sci. **35**, 135 (1985).
36. W.J. Swiatecki *et al.*, Acta Phys. Pol. B **34**, 2049 (2002).
37. B.B. Back, Phys. Rev. C **31**, 2104 (1985).
38. W. Loveland, in *Proceedings of the Sixth International Conference on Radioactive Nuclear Beams (RNB6), Argonne, Illinois, USA, 22-26 September 2003*, Nucl. Phys. A **746**, 108 (2004).
39. C.C. Sahm *et al.*, Nucl. Phys. A **441**, 316 (1985).
40. A.B. Quint *et al.*, Z. Phys. A **346**, 119 (1993).
41. A.M. Vinodkumar *et al.*, private communication.